RSC Chemical Biology

ROYAL SOCIETY OF CHEMISTRY

PAPER

View Article Online
View Journal

Cite this: DOI: 10.1039/d6cb00050a

A green enzymatic route for the biotransformation of naphthalene to phthalic acid

Yang Huang,†[ac] Maxine Yew,†[bc] Suxin Huang,[c] Haifeng Liu *[d] and Leilei Zhu *[bc]

Received 5th February 2026,
Accepted 3rd April 2026

DOI: 10.1039/d6cb00050a

rsc.li/rsc-chembio

Naphthalene, an abundant polycyclic aromatic hydrocarbon (PAH) often emitted as an industrial byproduct, represents a significant yet underutilized carbon feedstock for chemical synthesis. Due to its high chemical stability and hydrophobicity, conventional physicochemical treatment methods are often energy-intensive, condition-dependent, and prone to causing secondary pollution. Biocatalysis offers a green strategy for the selective activation and cleavage of aromatic rings under mild conditions. In this study, we constructed a multi-enzyme cascade reaction for the continuous biocatalytic conversion of naphthalene to phthalic acid. The cascade begins with the oxyfunctionalization of naphthalene into 1-naphthol by using the unspecific peroxygenase AaeUPO, followed by a carboxylation-oxygenation coupling reaction to yield 2′-carboxybenzyl-pyruvic acid, and ultimately an NAD^+-dependent oxidation to transform 2-carboxybenzaldehyde into phthalic acid. This work demonstrates a promising multi-enzyme strategy for the mild conversion of naphthalene and provides a methodological and conceptual basis for developing green and sustainable biotransformation routes for PAHs.

Introduction

Naphthalene ($C_{10}H_8$) is a carbon-rich polycyclic aromatic hydrocarbon massively produced as a byproduct of industrial processes such as petroleum refining, coal coking, and combustion. It poses significant risks to ecosystems and human health, including mutagenic, carcinogenic, and reproductive toxic effects.[1–3] Conventional treatments mainly rely on high-pressure hydrocracking.[4] While these methods can facilitate the rapid conversion of naphthalene, the associated processes are energy-intensive and involve rigorous operational conditions, producing complex byproducts. Such practices are inherently unsustainable, leading to irreversible carbon loss.

Instead of destroying the existing carbon framework, a more sustainable strategy is to valorize naphthalene into useful chemical building blocks through selective catalytic transformations. In recent years, biocatalysis has garnered significant interest as a green and selective approach to upcycling aromatic hydrocarbons.[5] Numerous PAH-utilizing bacteria have been identified, such as *Mycobacterium*, *Rhodococcus*, and *Nocardioides*.[6–8] In natural ecosystems, these microorganisms employ complex multi-enzyme systems, including dioxygenases, peroxidases, and monooxygenases, to facilitate regioselective hydroxylation and the subsequent ring-opening of PAHs into metabolic intermediates.[9–11] Despite this potential, practical applications of these biological pathways are limited by substrate hydrophobicity and recalcitrance of PAHs, slow enzymatic kinetics and inhibitory effects arising from toxic intermediates. To enable practical valorization, advances in genetic and protein engineering strategies are necessary, such as metabolic pathway optimization, targeted enhancement of enzyme activity and development of robust reaction systems.[12]

Among these processes, the initial oxyfunctionalization of naphthalene is key to downstream biotransformation steps. By introducing hydroxyl groups into the aromatic ring, the stable aromatic system is disrupted, thus enabling ring-cleavage reactions.[13] Unspecific peroxygenases (UPOs) are fungal-secreted heme-thiolate enzymes that catalyze oxygen-atom transfer using H_2O_2 as both the oxygen source and primary oxidant. Unlike traditional monooxygenases, they can hydroxylate aromatic rings and selectively oxidize alkanes without the requirement for complex external cofactors or auxiliary reductase proteins.[14–16] The high regioselectivity and operational simplicity with hydrophobic substrates make UPOs promising catalysts for the activation of PAHs. Oxidative activation of the otherwise inert aromatic ring generates more activated intermediates,

[a] College of Biotechnology, Tianjin University of Science and Technology, Tianjin, 300457, China
[b] State Key Laboratory of Engineering Biology for Low-Carbon Manufacturing, Tianjin, China
[c] Institute of Industrial Biotechnology, Chinese Academy of Sciences, 32 West 7th Avenue, Tianjin 300308, China. E-mail: zhu_ll@tib.cas.cn
[d] Jiangsu Collaborative Innovation Centre of Chinese Medicinal Resources Industrialization, School of Pharmacy, Nanjing University of Chinese Medicine, Nanjing 210023, China
† These authors contributed equally.

enabling downstream biocatalytic transformations, including hydroxylation, carboxylation, and ultimately ring cleavage by dioxygenases. Complementing this oxidative activation, cofactor-independent decarboxylases such as 2,3-dihydroxybenzoate decarboxylase, 2,6-dihydroxybenzoate decarboxylase, and salicylate decarboxylase, catalyze the efficient carboxylation of phenolic intermediates without external cofactors or energetic input.[17] Subsequently, aromatic ring-cleaving dioxygenases mediate the critical C–C bond-breaking step, producing ring-opened intermediates bearing carboxylated side chains that can serve as valuable building blocks for chemical synthesis.[18] Accordingly, reassembling these natural enzyme modules according to their thermodynamic and kinetic characteristics offers a viable approach to the construction of *in vitro* multi-enzyme cascades. For the biotransformation of naphthalene, this cell-free strategy offers advantages such as the flexibility to construct optimized non-metabolic routes bypassing the inherent constraints of cellular toxicity. Additionally, the modular nature of the *in vitro* cascade provides a clearer view into the efficiency of the reaction chain while allowing real-time tuning of enzymatic catalysts at different stages.

Building upon the one-pot enzymatic framework for the conversion of 1-naphthol into 2′-carboxybenzyl-pyruvic acid established previously by our group, the present study extends the pathway upstream through integrating the unspecific peroxygenase AaeUPO-catalyzed hydroxylation of naphthalene.[19] Furthermore, the cascade is further extended downstream to convert 2′-carboxybenzyl-pyruvic acid into phthalic acid, thereby establishing a complete *in vitro* multi-enzyme system for the full conversion of naphthalene to phthalic acid under mild conditions.

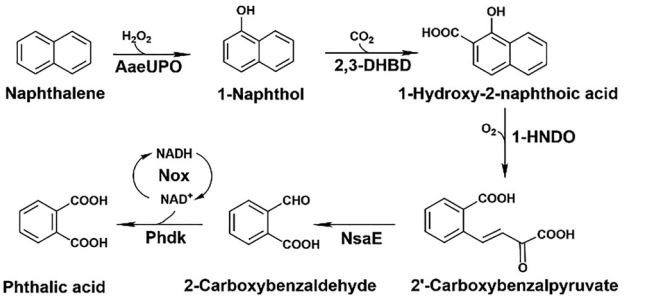

Scheme 1 Proposed multi-enzyme cascade for the bioconversion of naphthalene into phthalic acid. The pathway illustrates the sequential transformation of naphthalene into phthalic acid *via* key intermediates, including 1-naphthol, 1-hydroxy-2-naphthoic acid (1-H2NA), 2′-carboxybenzyl-pyruvic acid and 2-carboxybenzaldehyde. Enzymes involved: unspecific peroxygenase (AaeUPO), 2,3-dihydroxybenzoate decarboxylase (2,3-DHBD), dioxygenase (1-HNDO), 2-carboxybenzaldehyde dehydrogenase (Phdk), *trans-o*-hydroxybenzylidenepyruvate hydratase–aldolase (NsaE) and NADH oxidase (Nox).

Results and discussion

Design of a reaction route for naphthalene conversion to phthalic acid

In our previous work, we established a one-pot enzymatic cascade route for the transformation of 1-naphthol to 2′-carboxybenzyl-pyruvic acid *via* a cofactor-free carboxylation-oxygenation coupling reaction.[19] In this study, we extended the upstream process using 1-naphthol generated *in situ via* the AaeUPO-catalyzed oxidation of naphthalene. We subsequently expanded the downstream reaction pathway through the integration of Phdk dehydrogenase, which catalyzes the conversion of 2-carboxybenzylaldehyde into phthalic acid (Scheme 1).[20] In this synergistic pathway, 2,3-dihydroxybenzoate decarboxylase (2,3-DHBD) catalyzes the regioselective carboxylation of 1-naphthol to 1-hydroxy-2-naphthoic acid (1-H2NA), with 200 mM $KHCO_3$ supplied as the CO_2 source. 1-H2NA was subsequently subjected to oxidative ring cleavage by 1-hydroxy-2-naphthoate dioxygenase (1-HNDO) to produce 2′-carboxybenzyl-pyruvic acid. The carboxylation of 1-naphthol to 1-H2NA by 2,3-DHBD is the rate-limiting step due to the reaction's endothermic nature. However, coupling this step with the subsequent, highly exergonic downstream ring-opening reaction catalysed by the 1-HNDO dioxygenase provides a thermodynamic driving force that drives the carboxylation reaction forward, with the carboxylated intermediate quickly consumed to form 2′-carboxybenzyl-pyruvic acid (see Fig. S3). This intermediate was transformed to its aldehyde form catalyzed by *trans-o*-hydroxybenzylidenepyruvate hydratase–aldolase (NsaE), followed by 2-carboxybenzaldehyde dehydrogenase, Phdk-mediated oxidation to the final product, phthalic acid, while NADH oxidase (Nox) maintains redox sustainability through NAD^+ regeneration.[21,22] The study systematically evaluates key bottlenecks and synergistic effects within the cascade, providing a new green strategy and theoretical framework for the enzymatic transformation of complex PAHs.

Heterologous expression and assessment of AaeUPO oxyfunctionalization activity

The heterologous functional expression of UPOs and the corresponding product yields remains a key bottleneck for their scale-up application.[16] As a fungal-derived heme-thiolate protein, AaeUPO has been reportedly expressed in eukaryotic hosts such as *Saccharomyces cerevisiae* and *Pichia Pastoris*.[15,23] In this work, the reported AaeUPO (variant Jawa) was successfully expressed in *Saccharomyces cerevisiae* and secreted extracellularly. The activity of the AaeUPO (0.11 U mL^{-1}) was verified using an ABTS assay, where the enzyme utilizes hydrogen peroxide (H_2O_2) as the oxidant to catalyze the one-electron oxidation of ABTS.[24] Fig. 1A confirms the catalytic activity of the crude AaeUPO, showing a significant peroxidative activity towards ABTS compared to negative controls; Fig. 1B shows the mechanism of the ABTS assay for the confirmation of UPO peroxidative activity.

AaeUPO-catalyzed naphthalene hydroxylation to 1-naphthol

The regioselective hydroxylation of naphthalene was achieved using the functionally expressed crude AaeUPO. Acetonitrile (MeCN) was added as a co-solvent to enhance naphthalene solubility in the reaction system, and H_2O_2 as the requisite

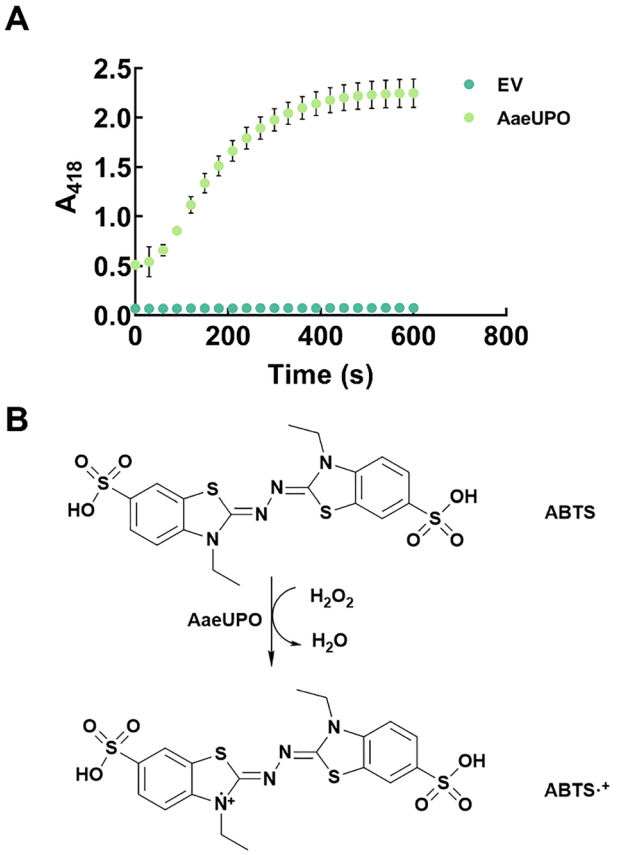

Fig. 1 Activity assessment of AaeUPO using ABTS assay. (A) Colorimetric response of the functionally expressed AaeUPO using the ABTS assay. EV represents the empty vector control, and AaeUPO represents *Agrocybe aegerita* unspecific peroxygenase. (B) ABTS assay for the confirmation of the peroxidative activity of UPO.

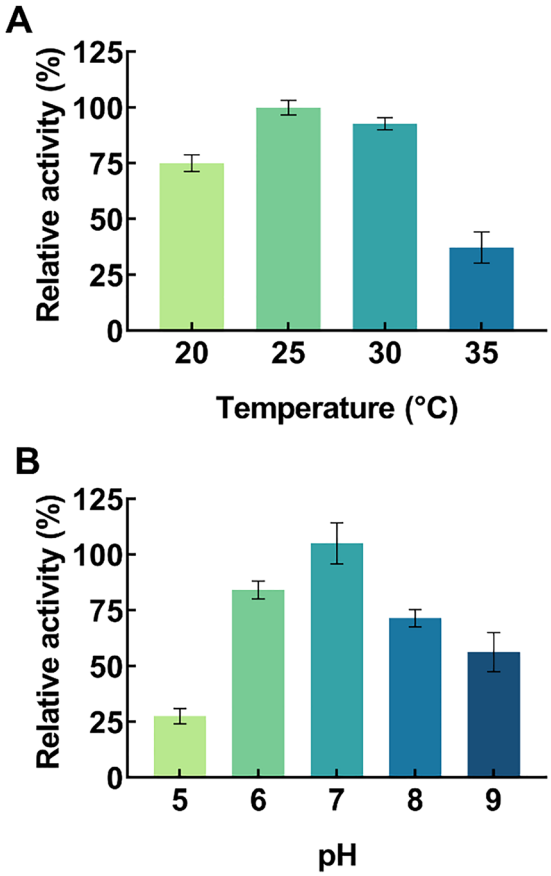

Fig. 2 Optimization of the reaction parameters for AaeUPO-catalyzed naphthalene hydroxylation. (A) Effect of temperature on catalytic activity. The optimal reaction temperature was evaluated using 1 mM naphthalene and 20% (v/v) acetonitrile. (B) Effect of pH on conversion efficiency. The optimal reaction pH was determined using 1 mM naphthalene and 20% (v/v) acetonitrile across a pH range of 5.0 to 9.0. All experiments were performed in duplicate (n = 2) and data are presented as the mean value.

oxygen donor. Before examining the interplay between substrate loading, organic solvent and peroxide inhibition, the reaction pH and temperature were first optimized to ensure the activity and stability of AaeUPO. Reactions were conducted over a pH range of 5.0 to 9.0 and at temperatures of 20 °C to 35 °C. As illustrated in Fig. 2, the highest product yields were achieved at pH 7.0 and 25 °C; notably, increasing the temperature beyond 25 °C resulted in a drastic drop of product yield, likely due to the limited thermal stability of the crude AaeUPO extract (Fig. 2A). AaeUPO exhibited its optimal catalytic activity and stability under neutral to slightly alkaline conditions, specifically at pH 7.0 (Fig. 2B). A significant decrease in the reaction rate was observed under acidic conditions, as the AaeUPO heme-thiolate center is prone to protonation which destabilizes the enzyme.[15]

In the AaeUPO catalytic cycle, H_2O_2 plays a dual role: it is the essential oxidant required to form the high-valent oxo-iron species for C–H bond activation of the naphthalene ring, yet it can also cause irreversible oxidative damage to the heme prosthetic group.[25,26] To balance catalytic productivity with enzyme stability, the effect of H_2O_2 concentration was investigated to identify the optimal threshold in this reaction. Despite the equimolar stoichiometric requirement for naphthalene hydroxylation, the impact of H_2O_2 concentration was evaluated at higher substrate loadings of 5 and 10 mM naphthalene to examine their effect on conversion efficiency (Fig. 3A). At 5 mM naphthalene loading, the maximum 1-naphthol yield was achieved with an equimolar (5 mM) H_2O_2, whereas a surplus of H_2O_2 at 10 mM resulted in a slight decline of yield, likely due to the onset of oxidative inactivation of the AaeUPO heme-thiolate center. The addition of 2 mM H_2O_2 produced the lowest yield, confirming that oxidant availability was the limiting factor. Interestingly, increasing the naphthalene concentration to 10 mM resulted in an overall lower yield, with the peak yield still occurring at 5 mM H_2O_2. We posit this to be due to the enzyme's sensitivity to peroxide, possible substrate inhibition due to the bulk of the hydrophobic naphthalene molecules, as well as the reaction system approaching its absolute limit of naphthalene solubility at 10 mM. Thus, the optimal H_2O_2 concentration was capped at 5 mM for the 5–10 mM substrate range.

The inherent hydrophobicity and low aqueous solubility of naphthalene constrained substrate loading in the reaction system, thereby significantly limiting the overall product formation.

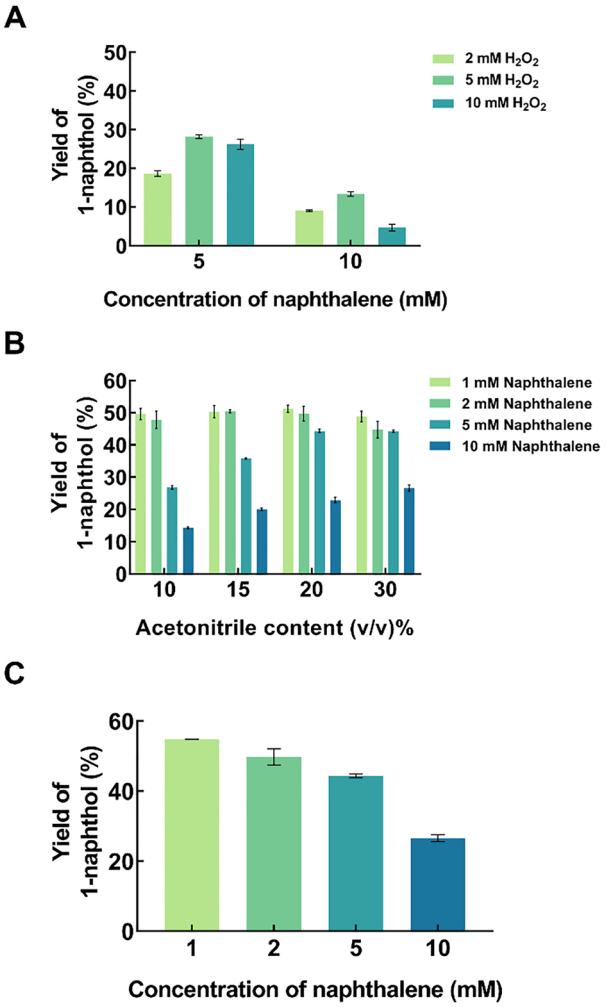

Fig. 3 Optimization of H_2O_2 and acetonitrile (MeCN) for naphthalene hydroxylation. (A) Impact of H_2O_2 dosage. Investigation of H_2O_2 concentration effects on the hydroxylation of naphthalene at varying initial naphthalene loadings. (B) Effects of MeCN concentration. Evaluation of the naphthalene conversion across different concentrations of naphthalene (1–10 mM) and MeCN amounts. (C) 1-Naphthol yields under optimized conditions. Final yields achieved using the optimized H_2O_2 dosage and MeCN amount for each naphthalene loading level. All experiments were performed in duplicate (n = 2), and error bars represent the standard deviation.

To address this limitation, acetonitrile (MeCN) was introduced as a co-solvent to enhance substrate solubility and promote a higher yield of 1-naphthol. Fig. 3B shows the production of 1-naphthol at varying concentrations of naphthalene (1, 2, 5 and 10 mM) and acetonitrile (10–30 vol%). H_2O_2 was added at a 1 : 1 molar ratio relative to the naphthalene concentration, except for reactions with 10 mM naphthalene, which were supplied with 5 mM H_2O_2. At lower naphthalene loading of 1 and 2 mM, no notable change of yield was observed when increasing the amount of MeCN from 10 to 20% (v/v). However, a gradual decline was noted when the amount of MeCN was increased to 30% (v/v), indicating the solvent-induced destabilization of the AaeUPO began to outweigh the benefits of the organic environment. Conversely, for the 10 mM naphthalene loading, the highest yield of 26.6% was achieved at 30% (v/v) MeCN; while increasing MeCN from 20 to 30% (v/v) has no impact on 5 mM naphthalene loading. While further increasing MeCN to 50% (v/v) effectively solubilized the naphthalene, it resulted in a reduced yield of 20.4% (see Fig. S2). This suggests that the reaction is primarily solubility-limited; nonetheless, increasing the portion of organic solvent beyond a critical threshold may lead to the displacement of essential water by MeCN molecules from the protein shells, which results in enzyme denaturation.[27] Fig. 3C presents the 1-naphthol yields across varying naphthalene loadings using the previously optimized H_2O_2 and acetonitrile concentration, with the maximum yield achieved at 1 mM naphthalene. In light of the aforementioned constraints, the subsequent downstream cascade reactions focused on naphthalene loadings within the 1 to 5 mM range.

A one-pot multi-enzyme cascade system for naphthalene conversion to phthalic acid

In our previous work, we demonstrated that the conversion of 1-naphthol into 2′-carboxybenzyl-pyruvic acid could achieve an overall yield of 78.5% at room temperature *via* cofactor-free carboxylation-oxygenation coupled reaction.[19] We extended this process by incorporating *trans-o*-hydroxybenzylidenepyruvate hydratase-aldolase (NsaE), 2-carboxybenzaldehyde dehydrogenase (Phdk) and NADH oxidase (Nox) into the one-pot cascade system, which enables the subsequent conversion of 2′-carboxybenzyl-pyruvic acid into phthalic acid. To systematically construct the multi-enzyme system, we adopted a stepwise approach: first optimizing the reaction conditions of the downstream cascade, then evaluating its catalytic efficiency using 1-naphthol as the substrate, and finally assessing the fully integrated cascade using naphthalene as the reaction feedstock. To determine the optimal reaction pH for the downstream module, the downstream reaction was systematically evaluated across a pH range of 4.0 to 7.0. As illustrated in Fig. 4A, using 5 and 10 mM 1-naphthol as the substrate, the optimal downstream reaction pH was identified from pH 6.0 to 7.0. This near-neutral range maximizes the catalytic efficiency while ensuring the structural stability of the enzymatic components. As shown in Fig. 4B, the multi-enzyme cascade was evaluated at 1-naphthol loadings of 5, 10 and 15 mM, with 2,3-DHBD, 1-HNDO, Phdk, NsaE and Nox loaded at a final concentration of 0.75 mg mL^{-1}. After a 12 hour reaction, a maximum yield of 78% phthalic acid was achieved at 5 mM 1-naphthol. At 10 mM and 15 mM 1-naphthol, the phthalic yields are 44% and 19%, respectively. We hypothesize the decline in yield at high substrate concentration is due to the inherent toxicity of 1-naphthol, which acts as a potent inhibitor of the downstream cascade, compromising the stability of other enzymes, thus preventing the system from achieving high conversion efficiency.

Having established that 1-naphthol can be successfully transformed into phthalic acid, we integrated the upstream oxidation of naphthalene into a one-pot cascade system. In this optimized configuration, all reaction components-including the naphthalene substrate, 20% (v/v) MeCN, AaeUPO, 2,3-DHBD, 1-HNDO, Phdk, NsaE, Nox, and 200 mM $KHCO_3$-were introduced

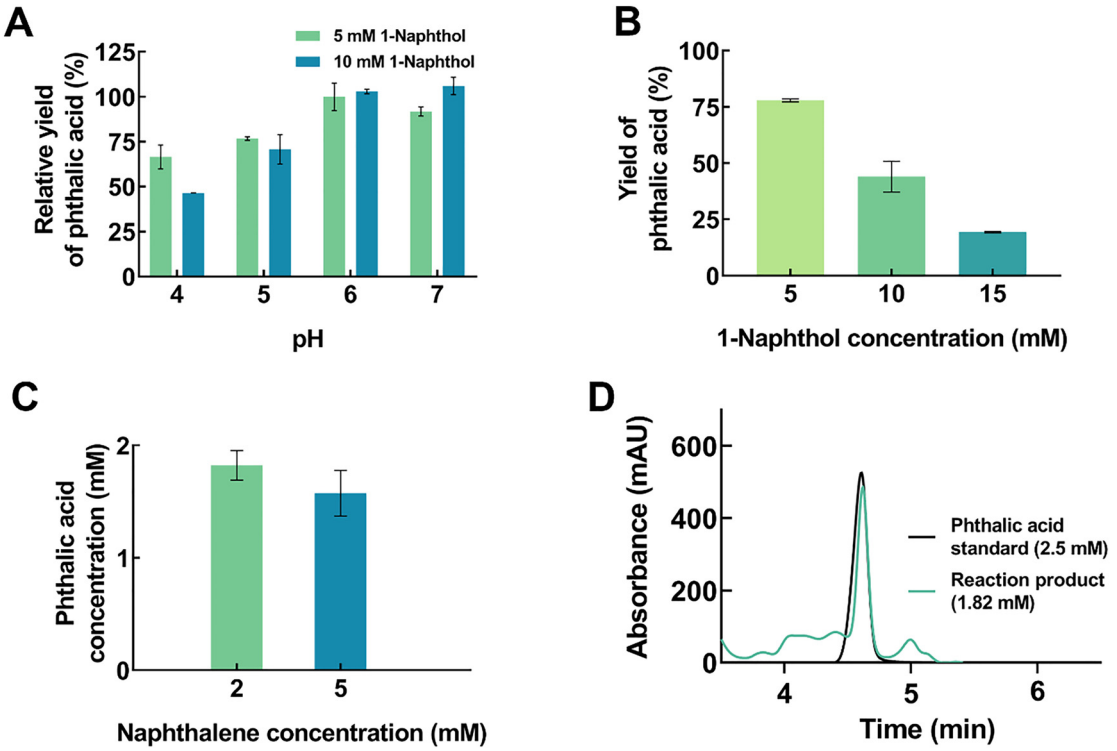

Fig. 4 A multi-enzyme cascade for the synthesis of phthalic acid. To systematically establish the system, a staged approach was adopted: first optimizing the downstream pathway (A) and evaluating its efficiency (B) using 1-naphthol as the starting substrate, followed by the evaluation of the fully integrated cascade using naphthalene (C) and (D). (A) Optimization of the reaction pH. The downstream reaction was evaluated using 5 mM and 10 mM 1-naphthol as reaction feedstock across a pH range of 4.0 to 7.0. The relative yield of phthalic acid (%) was calculated based on the maximum amount of phthalic acid formed, which was defined as 100%. Each enzyme (2,3-DHBD, 1-HNDO, Phdk, Nox and NsaE) was loaded at a final concentration of 0.75 mg mL^{-1}. (B) 1-Naphthol loading effects. Yield of phthalic acid across varying initial concentrations of 1-naphthol. (C) Effect of naphthalene loading on phthalic acid production. Comparison of phthalic acid concentrations (mM) obtained from the fully integrated cascade with initial naphthalene loadings of 2 mM and 5 mM. (D) Overlay of chromatograms comparing 2.5 mM phthalic acid standard (black) and the crude reaction product (green) from the one-pot multi-enzyme cascade. A final phthalic concentration of 1.82 mM was obtained with 2 mM naphthalene as the reaction feedstock, representing an overall molar yield of 91.2%. This confirms the enzymatic transformation of naphthalene into phthalic acid with a characteristic peak at 4.6 min. Reactions for (B) and (C) were performed at the optimized pH 7.0. All experiments were performed in duplicate (n = 2), and error bars represent the standard deviation.

simultaneously into a 1.0 mL reaction volume. The reaction was performed at naphthalene loadings of 2 and 5 mM, initiated by the addition of H_2O_2 and incubated for 12 hours. Using 2 mM naphthalene as the initial feedstock, 1.82 mM phthalic acid was obtained, corresponding to an overall molar yield of 91.2% phthalic acid. This high conversion suggests that the downstream ring-cleavage is an important driving force for the AaeUPO-mediated oxidation of naphthalene. As soon as 1-naphthol is formed, it is quickly consumed in the downstream carboxylation-oxygenation coupling reaction. Conversely, a further increase in the naphthalene concentration to 5 mM resulted in 1.57 mM phthalic acid, representing a molar yield of only 31.5% (Fig. 4C). This suggests that, while the system remains active, high substrate loadings may exert adverse inhibition on the enzymes. HPLC analysis (Fig. 4D) confirmed the formation of phthalic acid, identified by its characteristic peak at 4.6 min.

The limited efficiency of the full cascade is primarily attributed to two critical bottlenecks identified within the multi-enzyme cascade. The primary constraint is the relatively low conversion efficiency of the initial AaeUPO-catalyzed hydroxylation, as seen when the naphthalene loading is increased. As the gateway reaction, its limited efficiency restricts the flux of 1-naphthol into the downstream cleavage cascade, thereby capping the maximum attainable yield of the final product. A second bottleneck arises downstream, where the spontaneous decomposition of the intermediate 2′-carboxybenzyl-pyruvic acid into 2-carboxybenzaldehyde becomes rate-limiting under the current conditions. Ultimately, the limited conversion highlights the complex interplay of the multi-enzymatic components, which necessitates further optimizations to improve system compatibility and robustness. Nonetheless, our findings successfully demonstrated a feasible green route for the biotransformation of naphthalene into phthalic acid, providing a promising framework for converting petrochemical by-products into value-added chemicals.

Conclusions

This study demonstrates a one-pot, two-stage enzymatic cascade for the biotransformation of naphthalene into phthalic

acid. By coupling AaeUPO-catalyzed hydroxylation of naphthalene with a downstream carboxylation-oxygenation ring-cleavage pathway, we establish a green route for transforming a persistent aromatic byproduct from the petroleum industry into a valuable chemical building block. Despite this proof-of-concept, there remain two key limitations to the system's performance. First, the overall kinetics of the cascade reaction are constrained by the potent inhibitory effect of 1-naphthol on the other enzymes, which creates a kinetic bottleneck for the effective conversion to phthalic acid in the downstream pathway. Second, the naphthalene activation reaction is solubility-limited and prone to peroxidative stress, which could lead to enzymatic deactivation.

Future efforts should focus on the stability of the ''gateway'' naphthalene activation and the overall synchronization of the multi-enzyme cascade. In particular, protein engineering of UPO to improve polycyclic substrate affinity, solvent tolerance, and resistance to peroxidative inactivation is essential for achieving higher upstream conversion. In parallel, improved coordination of the downstream reactions is necessary to resolve the kinetics bottleneck arising from the accumulation of intermediates and to propel the ring-opening reaction forward. Together, these strategies could enhance the robustness of the multi-enzyme cascade.

Author contributions

Y. H: writing – original draft, visualization, validation, methodology, investigation, formal analysis, data curation. M. Y: writing – original draft, review and editing, visualization, validation, formal analysis, data curation. S. H: validation, investigation, methodology, data curation. H. Liu: writing – review and editing, supervision, conceptualization. L. Z: writing – review and editing, supervision, resources, project administration, funding acquisition, conceptualization.

Conflicts of interest

There are no conflicts to declare.

Data availability

The data supporting this article have been included as part of the supplementary information (SI). Supplementary information: Materials and methods, Tables S1–S5, Fig. S1–S3 and further experimental details. See DOI: https://doi.org/10.1039/d6cb00050a.

Acknowledgements

This work is funded by the Tianjin Major Science and Technology Projects and Engineering Programs (25ZXWCSY00320) and the International Partnership Program of the Chinese Academy of Sciences (306GJHZ2025003BS).

Notes and references

1 R. Preuss, J. Angerer and H. Drexler, *Int. Arch. Occup. Environ. Health*, 2003, **76**, 556–576.
2 M. Oliveira, K. Slezakova, C. Delerue-Matos, M. C. Pereira and S. Morais, *Environ. Int.*, 2019, **124**, 180–204.
3 F. Barbosa Jr, B. A. Rocha, M. C. O. Souza, M. Z. Bocato, L. F. Azevedo, J. A. Adeyemi, A. Santana and A. D. Campiglia, *J. Toxicol. Environ. Health, Part B*, 2023, **26**, 28–65.
4 G. C. Laredo, P. M. Vega Merino and P. S. Hernández, *Ind. Eng. Chem. Res.*, 2018, **57**, 7315–7321.
5 P. Molina-Espeja, M. Cañellas, F. J. Plou, M. Hofrichter, F. Lucas, V. Guallar and M. Alcalde, *ChemBioChem*, 2016, **17**, 341–349.
6 A. Imam, S. Kumar Suman, P. K. Kanaujia and A. Ray, *Bioresour. Technol.*, 2022, **343**, 126121.
7 C. He, Y. Li, C. Huang, F. Chen and Y. Ma, *Front. Microbiol.*, 2018, **9**, 2595.
8 S. Srivastava and M. Kumar, in *Sustainable Green Technologies for Environmental Management*, ed. S. Shah, V. Venkatramanan and R. Prasad, Springer Singapore, Singapore, 2019, pp. 111–139.
9 C. E. Cerniglia, *Biodegradation*, 1992, **3**, 351–368.
10 R. W. Eaton and P. J. Chapman, *J. Bacteriol.*, 1992, **174**, 7542–7554.
11 A. K. Haritash and C. P. Kaushik, *J. Hazard. Mater.*, 2009, **169**, 1–15.
12 M. Hobisch, D. Holtmann, P. Gomez de Santos, M. Alcalde, F. Hollmann and S. Kara, *Biotechnol. Adv.*, 2021, **51**, 107615.
13 T. Wu, J. Xu, W. Xie, Z. Yao, H. Yang, C. Sun and X. Li, *Front. Microbiol.*, 2018, **9**, 1087.
14 M. Kluge, R. Ullrich, C. Dolge, K. Scheibner and M. Hofrichter, *Appl. Microbiol. Biotechnol.*, 2009, **81**, 1071–1076.
15 P. Molina-Espeja, E. Garcia-Ruiz, D. Gonzalez-Perez, R. Ullrich, M. Hofrichter and M. Alcalde, *Appl. Environ. Microbiol.*, 2014, **80**, 3496–3507.
16 D. T. Monterrey, A. Menés-Rubio, M. Keser, D. Gonzalez-Perez and M. Alcalde, *Curr. Opin. Green Sustainable Chem.*, 2023, **41**, 100786.
17 C. Wuensch, S. M. Glueck, J. Gross, D. Koszelewski, M. Schober and K. Faber, *Org. Lett.*, 2012, **14**, 1974–1977.
18 W. Zhang, H. Li, S. H. H. Younes, P. Gómez de Santos, F. Tieves, G. Grogan, M. Pabst, M. Alcalde, A. C. Whitwood and F. Hollmann, *ACS Catal.*, 2021, **11**, 2644–2649.
19 P. Ren, Z. Tan, Y. Zhou, H. Tang, P. Xu, H. Liu and L. Zhu, *Green Chem.*, 2022, **24**, 4766–4771.
20 R.-H. Peng, A.-S. Xiong, Y. Xue, X.-Y. Fu, F. Gao, W. Zhao, Y.-S. Tian and Q.-H. Yao, *FEMS Microbiol. Rev.*, 2008, **32**, 927–955.
21 R. L. Stingley, A. A. Khan and C. E. Cerniglia, *Biochem. Biophys. Res. Commun.*, 2004, **322**, 133–146.
22 T. Iwabuchi and S. Harayama, *J. Bacteriol.*, 1997, **179**, 6488–6494.

23 P. Molina-Espeja, S. Ma, D. M. Mate, R. Ludwig and M. Alcalde, *Enzyme Microb. Technol.*, 2015, **73–74**, 29–33.
24 A. Kinner, K. Rosenthal and S. Lütz, *Front. Bioeng. Biotechnol.*, 2021, **9**, 705630.
25 J. Dong, E. Fernández-Fueyo, F. Hollmann, C. E. Paul, M. Pesic, S. Schmidt, Y. Wang, S. Younes and W. Zhang, *Angew. Chem., Int. Ed.*, 2018, **57**, 9238–9261.
26 W. Zhang, H. Liu, M. M. C. H. van Schie, P.-L. Hagedoorn, M. Alcalde, A. G. Denkova, K. Djanashvili and F. Hollmann, *ACS Catal.*, 2020, **10**, 14195–14200.
27 J. Martin-Diaz, P. Molina-Espeja, M. Hofrichter, F. Hollmann and M. Alcalde, *Biotechnol. Bioeng.*, 2021, **118**, 3002–3014.